

# Shape dependence and anisotropic finite-size scaling of the phase coherence of three-dimensional Bose-Einstein condensed gases

Giacomo Ceccarelli, Francesco Delfino, Michele Mesiti, and Ettore Vicari

*Dipartimento di Fisica dell'Università di Pisa and INFN, Largo Pontecorvo 3, I-56127 Pisa, Italy*

(Dated: September 29, 2018)

We investigate the equilibrium phase-coherence properties of Bose-condensed particle systems, focussing on their shape dependence and finite-size scaling (FSS). We consider three-dimensional (3D) homogeneous systems confined to anisotropic  $L \times L \times L_a$  boxes, below the BEC transition temperature  $T_c$ . We show that the phase correlations develop peculiar anisotropic FSS for any  $T < T_c$ , in the large- $L$  limit keeping the ratio  $\lambda \equiv L_a/L^2$  fixed. This phenomenon is effectively described by the 3D spin-wave (SW) theory. Its universality is confirmed by quantum Monte Carlo simulations of the 3D Bose-Hubbard model in the BEC phase. The phase-coherence properties of very elongated BEC systems,  $\lambda \gg 1$ , are characterized by a coherence length  $\xi_a \sim A_t \rho_s / T$  where  $A_t$  is the transverse area and  $\rho_s$  is the superfluid density.

PACS numbers: 03.75.Hh, 67.85.Hj, 03.75.Gg, 64.60.an

## I. INTRODUCTION

The low-temperature behavior of three-dimensional (3D) bosonic gases is characterized by the formation of a Bose-Einstein condensate (BEC), below a finite-temperature BEC phase transition. The phase coherence properties of cold atomic gases within the low-temperature BEC phase have been investigated by several experiments with cold atoms in harmonic traps, see, e.g., Refs. [1–10]. The coherence length turns out to be equal to the condensate size in generic 3D traps. However, very elongated harmonic traps may give rise to a substantial phase decoherence along the longer axial direction [5–7, 11, 12].

In this paper we study the equilibrium phase-coherence properties of homogeneous Bose-condensed particle systems, focussing on their shape dependence and finite-size scaling (FSS). We show that homogeneous BEC systems constrained within  $L \times L \times L_a$  boxes develop a peculiar anisotropic FSS (AFSS), in the large- $L$  limit keeping the ratio  $\lambda \equiv L_a/L^2$  fixed. This AFSS is effectively described by a 3D spin-wave (SW) theory, providing a quantitative description of the crossover from 3D box geometries to elongated effectively 1D systems. The phase-correlation properties of the 3D SW theory are expected to be universal, i.e., they are expected to apply to any condensed particle system, at any temperature below the BEC transition. In particular, for very elongated BEC systems ( $\lambda \gg 1$ ) our analysis confirms that the one-particle correlation function decays exponentially along the axial direction, with a coherence length proportional to the transverse area.

An interesting many-body system showing BEC is the 3D Bose-Hubbard (BH) Hamiltonian [13], which models

gases of bosonic atoms in optical lattices [14]. It reads

$$H = -t \sum_{\langle ij \rangle} (b_i^\dagger b_j + b_j^\dagger b_i) + \frac{U}{2} \sum_i n_i (n_i - 1) - \mu \sum_i n_i, \quad (1)$$

where  $b_i$  is a bosonic operator,  $n_i \equiv b_i^\dagger b_i$  is the particle density operator, and the sums run over the bonds  $\langle ij \rangle$  and the sites  $i$  of a cubic lattice. We set the hopping parameter  $t = 1$ , so that all energies are expressed in units of  $t$ . The phase diagram of 3D BH models and their critical behaviors have been much investigated, see e.g. Refs. [13, 15–19]. Their  $T$ - $\mu$  phase diagram, see for example Fig. 1, presents a finite-temperature BEC transition line, characterized by the accumulation of a macroscopic number of atoms in a single quantum state. The condensate wave function provides the complex order parameter of the BEC transition, whose critical behavior belongs to U(1)-symmetric XY universality class [20]. The BEC phase extends below the BEC transition line. The phase coherence properties are inferred from the one-particle correlation function

$$G(\mathbf{x}, \mathbf{y}) \equiv \langle b_{\mathbf{x}}^\dagger b_{\mathbf{y}} \rangle. \quad (2)$$

Its behavior, and the related momentum distribution, can be experimentally investigated by looking at the interference patterns of absorption images after a time-of-flight period in the large-time ballistic regime [21].

We present a numerical analysis of the space-coherence properties of the 3D hard-core BH model within its BEC phase, by quantum Monte Carlo (QMC) simulations. The results agree with the AFSS behaviors obtained within the 3D SW theory, supporting its universality.

The paper is organized as follows. In Sec. II we present the 3D SW theory that provides an effective description of the long-range phase correlations within the BEC phase, and show the emergence of a nontrivial AFSS behavior. In Sec. III we investigate the space coherence

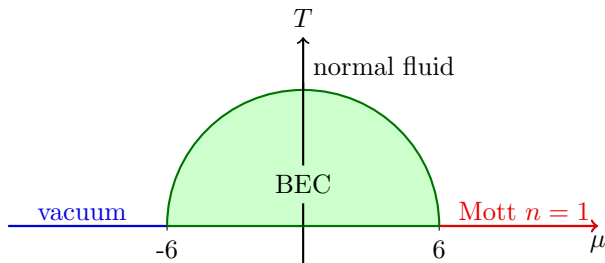


FIG. 1: (Color online) Sketch of the  $T$ - $\mu$  (in unit of the hopping parameter  $t$ ) phase diagram of the 3D BH model in the hard-core  $U \rightarrow \infty$  limit. The BEC phase is restricted to a finite region between  $\mu = -6$  and  $\mu = 6$ . It is bounded by a BEC transition line  $T_c(\mu)$ , which satisfies  $T_c(\mu) = T_c(-\mu)$  due to a particle-hole symmetry. Its maximum occurs at  $\mu = 0$ , where [18]  $T_c(\mu = 0) = 2.0160(1)$ . At  $T = 0$  two further quantum phases exist: the vacuum phase ( $\mu < -6$ ) and the incompressible  $n = 1$  Mott phase ( $\mu > 6$ ).

of the 3D hard-core BH model within its BEC phase by QMC simulations, confirming the universality of the AFSS behaviors obtained within the 3D SW theory. Finally, in Sec. IV we draw our conclusions. We also add an appendix containing some details of our numerical calculations.

## II. 3D SPIN-WAVE THEORY

Within the BEC phase, and for  $T \ll T_c$  when the density  $\rho_0 = \langle n_0 \rangle$  of the condensate is much larger than the density of the noncondensed atoms, the particle-field operator of homogeneous systems can be effectively approximated by [5]  $b(\mathbf{x}) = \sqrt{n_0} e^{i\theta(\mathbf{x})}$ . Then, the long-distance modes of the phase correlations are expected to be described by an effective 3D SW theory for a real phase field  $\theta(\mathbf{x})$ , which is invariant under a global shift  $\theta(\mathbf{x}) \rightarrow \theta(\mathbf{x}) + \varphi$ . The simplest SW action reads

$$S_{\text{sw}} = \int d^d x \frac{\alpha}{2} (\partial_\mu \theta)^2 \quad (3)$$

where  $\alpha$  plays the role of the superfluid density (as normally defined phenomenologically, [22]  $\alpha \propto \rho_s/T$ ). In the framework of the effective field theories [23], Eq. (3) represents the first non-trivial term of a derivative expansion of the fundamental field  $\theta(\mathbf{x})$ . Contributions of higher-order derivatives are expected to be suppressed in the long-range correlations. We return to this point later.

Actually, as argued in Ref. [5], the region where the SW theory effectively describes the long-distance phase correlations is expected to extend to the whole BEC phase, i.e. for  $T \lesssim T_c$ , excluding only the relatively small critical region close to  $T_c$ . This is essentially related to the fact that the fluctuations of the condensate density are suppressed below the critical region around  $T_c$ . Therefore, the two-point function

$$G_{\text{sw}}(\mathbf{x} - \mathbf{y}) = \langle e^{-i\theta(\mathbf{x})} e^{i\theta(\mathbf{y})} \rangle \quad (4)$$

is expected to describe the long-range phase-coherence properties of particle systems in the whole BEC phase.

We consider the 3D SW model in a finite box of generic shape  $L_1 \times L_2 \times L_3$  and periodic boundary conditions (PBCs). We regularize the theory on a corresponding  $L_1 \times L_2 \times L_3$  lattice, and write the partition function as

$$\begin{aligned} Z &= \sum_{\{n_\mu\}} \int D[\theta] e^{-\frac{\alpha}{2} \sum_{\mathbf{x}, \mu} (\theta_{\mathbf{x}} - \theta_{\mathbf{x}+\hat{\mu}} - 2\pi n_\mu \delta_{x_\mu L_\mu})^2} \\ &= \sum_{\{n_\mu\}} W(n_1, n_2, n_3) \int D[\theta] e^{-\frac{\alpha}{2} \sum_{\mathbf{x}, \mu} (\theta_{\mathbf{x}} - \theta_{\mathbf{x}+\hat{\mu}})^2} \\ &= \sum_{\{n_\mu\}} W(n_1, n_2, n_3) Z_0, \end{aligned} \quad (5)$$

where  $\mu = 1, 2, 3$ ,  $n_\mu \in \mathbb{Z}$ , the shift  $2\pi n_\mu \delta_{x_\mu L_\mu}$  at the boundary takes into account winding configurations on lattices with PBC, the weights  $W(n_\mu)$  are given by

$$\ln W = -2\pi^2 \alpha \left( \frac{L_2 L_3}{L_1} n_1^2 + \frac{L_3 L_1}{L_2} n_2^2 + \frac{L_1 L_2}{L_3} n_3^2 \right), \quad (6)$$

and  $Z_0$  is the plain partition function without shift at the boundaries. Analogous formulations of the SW theory have been considered to describe the quasi-long-range order of two-dimensional U(1)-symmetric systems [24–27].

The above formulas allow us to compute the helicity modulus along the three spatial directions, from the response of the system to a phase twisting  $\phi$  along one of the lattice directions [22]. We obtain

$$\begin{aligned} Y_1 &\equiv - \frac{L_1}{L_2 L_3} \left. \frac{\partial^2 \log Z(\phi)}{\partial \phi^2} \right|_{\phi=0} = \\ &= \alpha - 4\pi^2 \alpha^2 \frac{L_2 L_3}{L_1} \frac{\sum_{n=-\infty}^{\infty} n^2 e^{-2\pi^2 n^2 \alpha L_2 L_3 / L_1}}{\sum_{n=-\infty}^{\infty} e^{-2\pi^2 n^2 \alpha L_2 L_3 / L_1}} \end{aligned} \quad (7)$$

and analogously for  $Y_2$  and  $Y_3$ .

The two-point function (4) can be written as

$$\begin{aligned} G_{\text{sw}}(\mathbf{x} - \mathbf{y}) &= \langle e^{-i(\theta_{\mathbf{x}} - \theta_{\mathbf{y}})} \rangle_0 \\ &\times \frac{\sum_{\{n_\mu\}} W(n_\mu) \cos \left[ 2\pi \sum_{\mu=1}^3 n_\mu (x_\mu - y_\mu) / L_\mu \right]}{\sum_{\{n_\mu\}} W(n_\mu)}, \end{aligned} \quad (8)$$

where  $\langle \cdot \rangle_0$  denotes the expectation value in a Gaussian system without boundary shift (with PBC). Then we use the relation

$$\langle e^{-i(\theta_{\mathbf{x}} - \theta_{\mathbf{y}})} \rangle_0 = \exp[G_0(\mathbf{x}, \mathbf{y})] \quad (9)$$

where

$$\begin{aligned} G_0(\mathbf{x}, \mathbf{y}) &\equiv \langle (\theta_{\mathbf{x}} - \theta_{\mathbf{y}})^2 \rangle_0 \\ &= \frac{1}{\alpha L_1 L_2 L_3} \sum_{\mathbf{p} \neq 0} \frac{\cos[\mathbf{p} \cdot (\mathbf{x} - \mathbf{y})] - 1}{2 \sum_{\mu} (1 - \cos p_\mu)} \end{aligned} \quad (10)$$

with  $p_\mu = 2\pi\{0, \dots, L_\mu - 1\}/L_\mu$ . Eqs. (8-10) allow us to compute the  $G_{\text{sw}}(\mathbf{x})$  for any lattice shape and size. The

continuum limit is formally equivalent to the FSS limit, i.e.  $L_\mu \rightarrow \infty$  keeping appropriate ratios of the sizes fixed.

As already noted in Ref. [26], when we consider large-volume limits keeping the ratios of the sizes  $L_\mu$  finite, Eq. (7), and the analogous equations for the other directions, give equal helicity modulus. We obtain  $Y_\mu = \alpha$  for any  $\mu = 1, 2, 3$ . However, nontrivial results are obtained when considering elongated geometries, in particular when one size scales as the product of the sizes of the other two directions, giving rise to an AFSS.

Let us now consider the particular case of anisotropic geometries: we fix  $L_1 = L_2 = L$  and  $L_3 = L_a$ . More precisely, we consider the AFSS limit obtained by the large- $L$  limit at fixed ratio

$$\lambda \equiv L_a/L^2. \quad (11)$$

From Eq. (7) we obtain

$$Y_t = Y_1 = Y_2 = \alpha, \quad (12)$$

$$Y_a = Y_3 = \alpha - \frac{4\pi^2\alpha^2}{\lambda} \frac{\sum_{n=-\infty}^{\infty} n^2 e^{-2\pi^2 n^2 \alpha/\lambda}}{\sum_{n=-\infty}^{\infty} e^{-2\pi^2 n^2 \alpha/\lambda}}. \quad (13)$$

Therefore, the transverse helicity modulus  $\Upsilon_t \equiv TY_t$  can be again identified with the superfluid density. On the other hand,  $Y_a$  varies significantly with increasing  $\lambda$ , from  $Y_a = \alpha$  for  $\lambda \rightarrow 0$  to  $Y_a \rightarrow 0$  for  $\lambda \rightarrow \infty$ . Its AFSS can be written as

$$R_Y \equiv Y_a/Y_t = f_Y(\zeta), \quad \zeta \equiv Y_t/\lambda, \quad (14)$$

where

$$f_Y(\zeta) = 1 + 2\zeta \partial_\zeta \ln \vartheta_3(0|i2\pi\zeta), \quad (15)$$

and  $\vartheta_3(z|\tau)$  is the third elliptic theta function [28]. In particular,  $f_Y(0) = 0$  and  $f_Y(\infty) = 1$ . A plot of  $f_Y(\zeta)$  is shown in Fig. 2.

In the infinite-axial-size  $L_a \rightarrow \infty$  limit, the phase correlation  $G_{\text{sw}}(\mathbf{x})$  along the axial direction is essentially determined by the first factor of the r.h.s. of Eq. (8), since axial boundary terms become irrelevant, as indicated by the vanishing axial helicity modulus. In this limit  $G_{\text{sw}}(\mathbf{x})$  turns out to decay exponentially along the axial direction:

$$G_{\text{sw}}(0, 0, z \gg 1) \sim e^{-z/\xi_a} \quad (16)$$

(apart from a power-law prefactor), where

$$\xi_a = 2\alpha L^2. \quad (17)$$

This is obtained from the large-distance behavior of the Gaussian correlation (10):

$$G_0(0, 0, z \gg 1) \approx -\frac{z}{2\alpha L^2}. \quad (18)$$

In order to study the AFSS of the axial coherence length, we consider an alternative axial second-moment

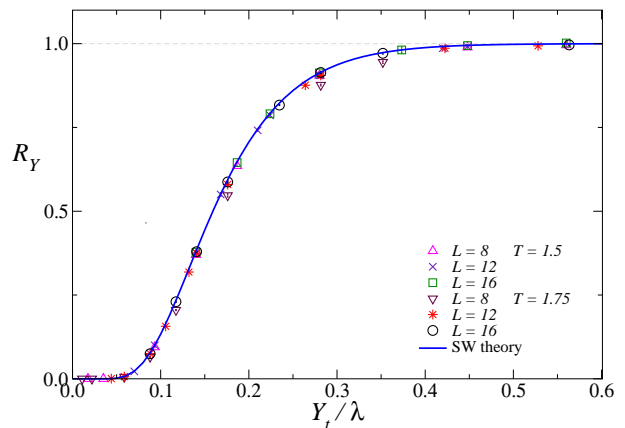


FIG. 2: (Color online) The ratio  $R_Y \equiv Y_a/Y_t$  for anisotropic  $L^2 \times L_a$  lattices with PBC, versus  $Y_t/\lambda$  where  $\lambda \equiv L_a/L^2$ . We show the curve (15) obtained by the 3D SW theory (full line), and QMC data for the 3D hard-core BH model, for  $\mu = 0$  and two temperature values, i.e.  $T = 1.5$  and  $T = 1.75$  (we use the QMC estimates  $Y_t \approx 0.280$  and  $Y_t \approx 0.176$  respectively). The MC data clearly approach the SW AFSS curve with increasing  $L$  (the differences get rapidly suppressed, apparently as  $L^{-3}$ ).

correlation length, as defined in Eq. (A2). We numerically compute it using Eqs. (8-10), for increasing values of  $L$  keeping  $\lambda = L_a/L^2$  fixed, up to values of  $L$  where the results become stable with great accuracy (lattice sizes  $L \gtrsim 10$  turn out to be sufficient to get a satisfactory  $O(10^{-5})$  accuracy for the large- $L$  limit). The results show that its AFSS can be written as

$$\xi_a(\lambda) \approx L_a \tilde{f}_\xi(\zeta) = 2Y_t L^2 f_\xi(\zeta) \quad (19)$$

with  $\zeta$  defined as in Eq. (14). Again,  $\tilde{f}_\xi$  and  $f_\xi$  are scaling functions. In particular  $\tilde{f}_\xi(0) = 0$  and  $f_\xi(0) = 1$  [29]. The scaling function  $f_\xi$  is shown in Fig. 3.

We also report the two-point function  $G_{\text{sw}}(\mathbf{x}, \mathbf{y})$  in the case of open boundary conditions (OBCs), where winding effects do not arise, but translation invariance is violated by the boundaries. Assuming that the site coordinates are  $x_\mu = [-(L_\mu - 1)/2, \dots, (L_\mu - 1)/2]$ ,

$$G_{\text{sw}}(\mathbf{x}, \mathbf{y})_{\text{obc}} = \exp\left(\frac{2M_{\mathbf{xy}} - M_{\mathbf{xx}} - M_{\mathbf{yy}}}{2\alpha}\right), \quad (20)$$

$$M_{\mathbf{xy}} = \sum_{\mathbf{p} \neq 0} 2^{n_p} \frac{\prod_\mu \cos[p_\mu(x_\mu + L_\mu/2)] \cos[p_\mu(y_\mu + L_\mu/2)]}{2L_1 L_2 L_3 \sum_\mu (1 - \cos p_\mu)}$$

with  $p_\mu = \pi\{0, \dots, L_\mu - 1\}/L_\mu$  and  $n_p$  is the number of momentum components different from zero. Analogously to the PBC case, for elongated  $L^2 \times L_a$  lattices with  $L_a \rightarrow \infty$ , the phase correlation asymptotically behaves as  $G_{\text{sw}}(0, 0, z \gg 1)_{\text{obc}} \sim e^{-z/\xi_a}$  with  $\xi_a$  given by Eq. (17).

Finally, assuming the universality of the above asymptotic AFSS for any BEC system, we would like to get information on the size of the corrections when approaching this universal limit. Corrections to the asymptotic scaling behavior are generally expected in generic BEC systems due to the fact that the corresponding effective SW

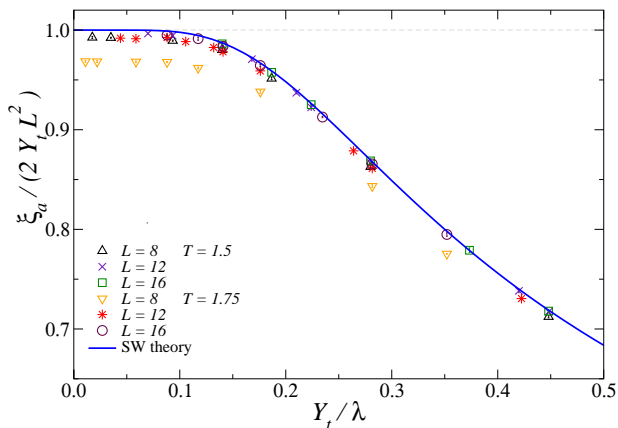


FIG. 3: (Color online) The ratio  $\xi_a/(2Y_tL^2)$ , where  $\xi_a$  is axial second-moment correlation length defined in Eq. (A2), versus  $Y_t/\lambda$  with  $\lambda \equiv L_a/L^2$ . We show results from the SW theory, and QMC data for the 3D hard-core BH model for  $\mu = 0$ , on  $L^2 \times L_a$  lattices with PBC (we use the QMC estimates  $Y_t \approx 0.280$  and  $Y_t \approx 0.176$  respectively for  $T = 1.5$  and  $T = 1.75$ ). The QMC data clearly approach the spin-wave AFSS with increasing  $L$  (the differences get rapidly suppressed, apparently as  $L^{-3}$ ).

theories generally require further higher-order derivative terms. Since the SW action (3) is quadratic, the power law of their suppression can be inferred by a straightforward dimensional analysis of the couplings of the further irrelevant higher-order derivative terms which are consistent with the global symmetries. Therefore, in the FSS or AFSS limit, their contributions are generally suppressed by  $O(L^{-2})$ , due to the fact that the next-to-leading terms has two further derivatives, and therefore the corresponding couplings have a square length dimension. Therefore, we expect that BEC systems rapidly approach the universal AFSS described by the SW quadratic theory. Notice that, in the presence of nontrivial boundaries,  $O(L^{-1})$  corrections may arise from boundary contributions.

### III. SPACE COHERENCE IN THE BEC PHASE OF THE 3D BH MODEL

In order to check the universality of the AFSS behavior of the phase correlations of the 3D SW theory, we consider the 3D BH model (1) in the hard-core  $U \rightarrow \infty$  limit and at zero chemical potential  $\mu = 0$ , on elongated  $L^2 \times L_a$  lattices with PBC. We present numerical results for a few values of the temperatures below the BEC phase transition occurring at [18]  $T_c \approx 2.0160$ , in particular  $T = 1.5$  and  $T = 1.75$  (which are both smaller than, but not far from,  $T_c$ ), obtained by QMC simulations. Some details are reported in App. A, with the definitions of the observables considered.

At  $\mu = 0$  the particle density of the hard-core BH model is exactly one half,  $\rho = \langle n_{\mathbf{x}} \rangle = 1/2$ , independently of  $T$  due to the particle-hole symmetry. More-

over, the on-site density fluctuation is exactly given by  $\langle n_{\mathbf{x}}^2 \rangle - \langle n_{\mathbf{x}} \rangle^2 = 1/4$ . The connected density-density correlation  $G_n(\mathbf{x})$ , cf. Eq. (A8), turns out to differ significantly from zero only at a distance of one lattice spacing, where it has a negative value, while it is strongly suppressed at larger distances, independently of the lattice size and shape. The corresponding values of the compressibility  $\kappa = \sum_{\mathbf{x}} G_n(\mathbf{x})$  are  $\kappa = 0.1172(1)$  and  $\kappa = 0.1407(1)$  respectively at  $T = 1.5$  and  $T = 1.75$ . Therefore, as expected, the observables related to the particle density do not show any relevant finite-size dependence within the BEC phase. As we shall see, other observables related to the phase correlations show a more interesting behavior.

Let us first consider the helicity modulus computed from the response of the system to a phase-twisting field along one of the directions [22], see App. A. In the case of bosonic systems and for homogeneous cubic-like systems, it is related to the superfluid density: [22]  $\Upsilon(T) \propto \rho_s(T)$ , thus  $\Upsilon(T)$  approaches a nonzero finite value for  $T \rightarrow 0$ .

However, for anisotropic  $L^2 \times L_a$  systems we must distinguish two helicity modulus along the transverse and axial directions:  $\Upsilon_t \equiv TY_t$  and  $\Upsilon_a \equiv TY_a$  from twisting along the transverse and axial directions respectively, cf. Eqs. (A4) and (A6). Their behaviors appear analogous to those obtained for the 3D SW theory in elongated geometries. Indeed, the QMC data at both  $T = 1.5$  and  $T = 1.75$  show that  $Y_t$  is stable with respect to variations of  $\lambda = L_a/L^2$ , while  $Y_a$  significantly decreases when increasing  $\lambda$ . Straightforward large- $L$  extrapolations of the finite- $L$  data lead to the estimates  $Y_t = 0.280(1)$  at  $T = 1.5$  and  $Y_t = 0.176(1)$  at  $T = 1.75$ .

The QMC data for the ratio  $R_Y \equiv Y_a/Y_t$  behave consistently with the AFSS behavior (14) of the 3D SW model. They are shown in Fig. 2. With increasing  $L$ , the data plotted versus  $Y_t/\lambda$  rapidly approach the SW curve for both temperatures  $T = 1.5$  and  $T = 1.75$ , supporting the universality of the SW results. Note that the temperature dependence enters only through the temperature dependence of the transverse helicity modulus  $Y_t$ .

The convergence of the QMC data to the asymptotic universal curve is apparently characterized by an  $O(L^{-3})$  approach, which is a higher power than the typical  $O(L^{-2})$  corrections expected in SW effective theories, see the discussion at the end of Sec. II. This may be explained by the fact that we are considering observables related to the axial size that scales as  $L^2$  in the AFSS limit. Thus, in the derivative expansion of the corresponding effective SW effective theory, a further derivative with respect to the axial space coordinate formally leads to a further power  $L^{-2}$ , instead of  $L^{-1}$ .

We also consider the axial second-moment correlation length  $\xi_a$ , defined in Eq. (A2). Again, its large- $L$  behavior is consistent with the AFSS obtained within the SW theory, cf. Eq. (19), as clearly demonstrated by the QMC data shown in Fig. 3.

Finally, we consider the space dependence of the two-point function along the axial direction, and, in particu-

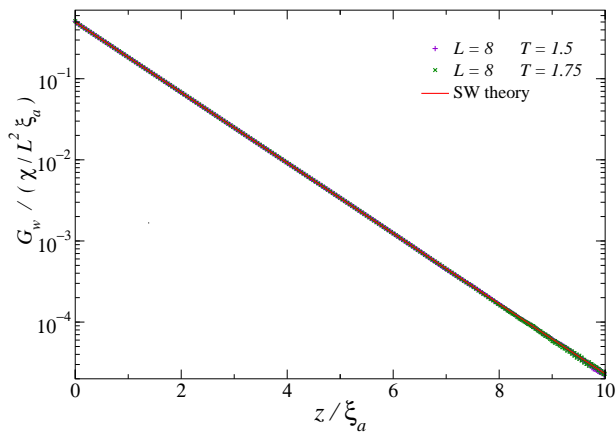


FIG. 4: (Color online) The wall-wall phase correlation  $G_w(z)$ , cf. Eq. (A3), in the infinite axial-size limit  $\lambda \rightarrow \infty$ . Again, the QMC data for the hard-core BH model and the computations using the 3D SW theory perfectly agree (actually their differences are hardly visible). Clearly,  $G_w(z)$  decays exponentially, as  $e^{-z/\xi_a}$  with  $\xi_a = 2Y_t L^2$ .

lar, of the axial wall-wall correlation defined in Eq. (A3). We expect that its AFSS reads

$$G_w(z) = \frac{\chi}{L^2 \xi_a} f_w(z/\xi_a, Y_t/\lambda) \quad (21)$$

where  $\chi$  is the spatial integral of  $G$ . In Fig. 4 we show QMC data in the infinite axial-size limit, i.e.  $\lambda \rightarrow \infty$  (obtained by increasing  $L_a$  at fixed  $L$ , up to the point the data become stable within errors). Again the QMC data nicely agree with the corresponding space dependence of the SW two-point function, obtained using formulas (8)-(10). In particular, they confirm the large-distance exponential decay with axial correlation length  $\xi_a = 2Y_t L^2$ , in agreement with Eqs. (17) and (19).

#### IV. CONCLUSIONS

We have studied the equilibrium phase-coherence properties of Bose-condensed particle systems, focussing on their shape dependence and FSS. In particular, we consider anisotropic  $L^2 \times L_a$  geometries with PBC, in the AFSS limit  $L \rightarrow \infty$  keeping the ratio  $\lambda \equiv L_a/L^2$  fixed.

The long-range phase-coherence properties of the BEC phase are effectively described by a 3D SW theory, which allows us to compute the asymptotic AFSS of the phase correlations. Such a behavior is universal, in particular it is independent of  $T$ . Indeed the temperature dependence enters only through a normalization of the scaling variable  $\lambda$ , which can be related to the helicity modulus  $\Upsilon_t$  along the transverse directions of size  $L$ . Phase decoherence occurs in the limit of very elongated systems, where the axial coherence length  $\xi_a$  remains finite in the limit  $\lambda \gg 1$ , and proportional to the transverse area. In particular, in the case of PBC and for  $\lambda \rightarrow \infty$ , we obtain  $\xi_a = 2L^2 \Upsilon_t / T$ . Since the transverse helicity modulus

maintains its correspondence with the superfluid density, i.e.  $\Upsilon_t \propto \rho_s$ , this relation may be turned into

$$\xi_a \propto \frac{\rho_s}{T} A_t, \quad (22)$$

where  $A_t$  is the transverse area.

To check the universality of the AFSS of the phase correlations, we consider the 3D BH lattice model (1), which models gases of bosonic atoms in optical lattices [21]. We present a numerical analysis in the hard-core  $U \rightarrow \infty$  limit based on QMC simulations within the BEC phase. The results confirm the universality of the AFSS described by the 3D SW theory. We stress that analogous behaviors are expected for finite on-site couplings  $U$ , and for generic BEC systems not constrained by a lattice structure.

The main features of the AFSS of anisotropic systems with PBC are expected to extend to other boundary conditions (appropriate to quantum many-body systems), in particular to the case of open boundary conditions (OBCs) which are more realistic for experimental setup. For example, in the infinite-axial-size limit and for OBC along all directions, the two-point correlation function of 3D SW model, cf. Eq. (20), shows an exponential decay along the axial direction as well. Analogously to the PBC case, the axial correlation length behaves as in Eq. (22).

An analogous space-decoherence phenomenon has been put forward for inhomogeneous atomic systems within elongated harmonic traps [5]. The bosonic systems in harmonic traps were studied assuming the Thomas-Fermi approximation for the space dependence of the particle density, and a Gaussian theory for the phase fluctuations [5]. Corresponding experimental evidence for the BEC of harmonically trapped  $^{87}\text{Rb}$  atoms has been also reported [6, 7]. The crossover from 3D BEC systems to the effectively 1D phase-fluctuating condensate regime has been also discussed for ring-shaped traps at  $T \ll T_c$ , using an approach based on the Gross-Pitaevskii equation [11], leading to analogous coherence properties in the limit of very elongated systems.

We finally note that our results for homogeneous BEC phases should also be of experimental relevance, since cold-atom systems constrained by effectively homogeneous traps have been recently realized [30].

It is worth mentioning that AFSS scenarios analogous to those of 3D BEC systems are also expected in generic 3D  $O(N)$ -symmetric statistical systems, such as 3D  $N$ -vector models, within their low-temperature phase where a spatially uniform magnetic field drives first-order transitions [31, 32] (in BEC systems an external field coupled to the condensation order parameter is not physical).

#### Acknowledgments

We acknowledge interesting and useful discussions with Enore Guadagnini and Mihail Mintchev.

## Appendix A: Quantum Monte Carlo simulations of the 3D BH model and observables

In our numerical study of the 3D BH model (1), we present results obtained by QMC simulations of the BH model in the hard-core  $U \rightarrow \infty$  limit, for temperature values  $T < T_c$ , on anisotropic  $L^2 \times L_a$  lattices with PBC, for various values of  $L$  (generally up to  $L = 16$ ) and  $L_a$ . We use the directed operator-loop algorithm, [33–35] which is a particular algorithm using the stochastic series expansion method.

The decay of phase coherence along the axial direction can be quantified by the one-particle correlation (2). The corresponding length scale  $\xi_a$  may be extracted from its exponential decay or its second moment along the axial direction. In the case of PBC translational invariance implies  $G(\mathbf{x} - \mathbf{y}) \equiv G(\mathbf{x}, \mathbf{y}) \equiv \langle b_{\mathbf{x}}^\dagger b_{\mathbf{y}} \rangle$ . We define its zero-momentum component

$$\chi = \sum_{\mathbf{x}} G(\mathbf{x}) \quad (\text{A1})$$

and the axial second-moment correlation length as

$$\xi_a^2 \equiv \frac{1}{4 \sin^2(\pi/L_a)} \left( \frac{\tilde{G}(\mathbf{0})}{\tilde{G}(\mathbf{p}_a)} - 1 \right), \quad (\text{A2})$$

where  $\tilde{G}(\mathbf{p})$  is the Fourier transform of  $G(\mathbf{x})$  and  $\mathbf{p}_a = (0, 0, 2\pi/L_a)$ . Moreover, we consider the wall-wall correlation function along the axial direction, defined as

$$G_w(z) \equiv \frac{1}{L^2} \sum_{x_1, x_2} G(x_1, x_2, z). \quad (\text{A3})$$

The helicity modulus  $\Upsilon$  is a measure of the response of the system to a phase-twisting field along one of the lattice directions [22]. In the case of bosonic systems and for homogeneous cubic-like systems, it is related to the superfluid density:  $\Upsilon(T) \propto \rho_s(T)$ . However, for anisotropic  $L^2 \times L_a$  systems we must distinguish two helicity modulus along the transverse and axial directions. In our QMC with PBC they can be estimated from the linear winding number  $W_t$  and  $W_a$  along the transverse and axial directions respectively. Therefore, we define transverse and axial helicity modulus:

$$\Upsilon_t \equiv \frac{1}{L_a} \left. \frac{\partial^2 F(\phi_t)}{\partial \phi_t^2} \right|_{\phi_t=0} = TY_t, \quad (\text{A4})$$

$$\Upsilon_a \equiv \frac{L_a}{L^2} \left. \frac{\partial^2 F(\phi_a)}{\partial \phi_a^2} \right|_{\phi_a=0} = TY_a, \quad (\text{A5})$$

$$Y_t \equiv \frac{1}{L_a} \langle W_t^2 \rangle, \quad Y_a \equiv \frac{L_a}{L^2} \langle W_a^2 \rangle, \quad (\text{A6})$$

where  $F = -T \ln Z$  is the total free energy,  $\phi_t$  and  $\phi_a$  are twist angles along one of the transverse directions and along the axial direction respectively.

We also consider the particle density  $\rho = \langle n_{\mathbf{x}} \rangle$ , and the compressibility

$$\kappa \equiv \frac{\partial \rho}{\partial \mu} = \frac{1}{V} \sum_{\mathbf{x}, \mathbf{y}} G_n(\mathbf{x}, \mathbf{y}), \quad (\text{A7})$$

$$G_n(\mathbf{x}, \mathbf{y}) \equiv \langle n_{\mathbf{x}} n_{\mathbf{y}} \rangle - \langle n_{\mathbf{x}} \rangle \langle n_{\mathbf{y}} \rangle. \quad (\text{A8})$$

- 
- [1] M. R. Andrews, C. G. Townsend, H.-J. Miesner, D. S. Durfee, D. M. Kurn, and W. Ketterle, Observation of Interference Between Two Bose Condensates, *Science* **275**, 637 (1997).
- [2] J. Stenger, S. Inouye, A. P. Chikkatur, D. M. Stamper-Kurn, D. E. Pritchard, and W. Ketterle, Bragg Spectroscopy of a Bose-Einstein Condensate, *Phys. Rev. Lett.* **82**, 4569 (1999).
- [3] E. W. Hagley, L. Deng, M. Kozuma, M. Trippenbach, Y. B. Band, M. Edwards, M. Doery, P. S. Julienne, K. Helmerson, S. L. Rolston, and W. D. Phillips, Measurement of the coherence of a Bose-Einstein condensate, *Phys. Rev. Lett.* **83**, 3112 (1999).
- [4] I. Bloch, T.W. Hänsch, and T. Esslinger, Measurement of the spatial coherence of a trapped Bose gas at the phase transition, *Nature* **403**, 166 (2000).
- [5] D. S. Petrov, G. V. Shlyapnikov, and J. T. M. Walraven, Phase-fluctuating 3D Bose-Einstein condensates in elongated traps, *Phys. Rev. Lett.* **87**, 050404 (2001).
- [6] S. Dettmer, D. Hellweg, P. Ryytty, J. J. Arlt, W. Ertmer, K. Sengstock, D. S. Petrov, G. V. Shlyapnikov, H. Kreutzmann, L. Santos, and M. Lewenstein, Observation of Phase Fluctuations in elongated Bose-Einstein Condensates, *Phys. Rev. Lett.* **87**, 160406 (2001).
- [7] D. Hellweg, S. Dettmer, P. Ryytty, J. J. Arlt, W. Ertmer, K. Sengstock, D. S. Petrov, G. V. Shlyapnikov, H. Kreutzmann, L. Santos, and M. Lewenstein, Phase Fluctuations in Bose-Einstein Condensates, *Appl. Phys. B* **73**, 781 (2001).
- [8] L. Cacciapuoti, D. Hellweg, M. Kottke, T. Schulte, K. Sengstock, W. Ertmer, J. J. Arlt, L. Santos, and M. Lewenstein, Second Order Correlation Function of a Phase Fluctuating Bose-Einstein Condensate, *Phys. Rev. A* **68**, 053612 (2003).
- [9] D. Hellweg, L. Cacciapuoti, M. Kottke, T. Schulte, K. Sengstock, W. Ertmer, and J. J. Arlt, Measurement of the Spatial Correlation Function of Phase Fluctuating Bose-Einstein Condensates, *Phys. Rev. Lett.* **91**, 010406 (2003).
- [10] S. Ritter, A. Öttl, T. Donner, T. Bourdel, M. Köhl, and T. Esslinger, Observing the Formation of Long-Range Order during Bose-Einstein Condensation, *Phys. Rev. Lett.* **98**, 090402 (2007).
- [11] L. Mathey, A. Ramanathan, K. C. Wright, S. R. Muniz, W. D. Phillips, and C. W. Clark, Phase fluctuations in anisotropic Bose-Einstein condensates: From cigars to rings, *Phys. Rev. A* **82**, 033607 (2010).
- [12] D. Gallucci, S. P. Cockburn, and N. P. Proukakis, Phase

- coherence in quasicondensate experiments: An *ab initio* analysis via the stochastic Gross-Pitaevskii equation, Phys. Rev. A **86**, 013627 (2012).
- [13] M.P.A. Fisher, P.B. Weichman, G. Grinstein, and D.S. Fisher, Boson localization and the superfluid-insulator transition, Phys. Rev. B **40**, 546 (1989).
- [14] D. Jaksch, C. Bruder, J.I. Cirac, C.W. Gardiner, and P. Zoller, Cold Bosonic Atoms in Optical Lattices, Phys. Rev. Lett. **81**, 3108 (1998).
- [15] B. Capogrosso-Sansone, N.V. Prokof'ev, and B.V. Svistunov, Phase diagram and thermodynamics of the three-dimensional Bose-Hubbard model, Phys. Rev. B **75**, 134302 (2007).
- [16] J. Carrasquilla and M. Rigol, Superfluid to normal phase transition in strongly correlated bosons in two and three dimensions, Phys. Rev. A **86**, 043629 (2012).
- [17] G. Ceccarelli, C. Torrero, and E. Vicari, Critical parameters from trap-size scaling in trapped particle systems, Phys. Rev. B **87** 024513 (2013).
- [18] G. Ceccarelli and J. Nespolo, Universal scaling of three-dimensional bosonic gases in a trapping potential, Phys. Rev. B **89**, 054504 (2014).
- [19] G. Ceccarelli, J. Nespolo, A. Pelissetto, and E. Vicari, Bose-Einstein condensation and critical behavior of two-component bosonic gases, Phys. Rev. A **92**, 043613 (2015); Phase diagram and critical behaviors of mixtures of Bose gases, Phys. Rev. A **93**, 033647 (2016).
- [20] A. Pelissetto and E. Vicari, Critical Phenomena and Renormalization Group Theory, Phys. Rep. **368**, 549 (2002).
- [21] I. Bloch, J. Dalibard, and W. Zwerger, Many-body physics with ultracold gases, Rev. Mod. Phys. **80**, 885 (2008).
- [22] M. E. Fisher, M. N. Barber, and D. Jasnow, Helicity modulus, superfluidity, and scaling in isotropic systems, Phys. Rev. A **8**, 1111 (1973).
- [23] E. Weinberg, *The Quantum Theory of Fields* (Cambridge University Press, 1995).
- [24] M. Hasenbusch, The two dimensional XY model at the transition temperature: a high precision numerical study, J. Phys. A **38**, 5869 (2005).
- [25] M. Hasenbusch, A. Pelissetto, and E. Vicari, Multicritical behavior in the fully frustrated XY model and related systems, J. Stat. Mech. (2005) P12002.
- [26] N. V. Prokof'ev and B. V. Svistunov, Two definitions of superfluid density, Phys. Rev. B **61**, 11282 (2000).
- [27] R. G. Melko, A. W. Sandvik, and D. J. Scalapino, Aspect-ratio dependence of the spin stiffness of a two-dimensional XY model, Pgts. Rev. B **69**, 014509 (2004).
- [28] E. T. Whittaker and G. N. Watson, *A course of modern analysis*, Cambridge University Press, fourth edition, 1927.
- [29] Although the second-moment correlation length generally differs from that obtained from the large-distance exponential decay, they are expected to be equal for Gaussian-like theory, as supported by the direct computations at fixed  $L$  and  $L_a \rightarrow \infty$ .
- [30] N. Navon, A. L. Gaunt, R. P. Smith, and Z. Hadzibabic, Critical Dynamics of Spontaneous Symmetry Breaking in a Homogeneous Bose gas, Science **347**, 167 (2015).
- [31] M. E. Fisher and V. Privman, First-order transitions breaking  $O(n)$  symmetry: Finite-size scaling, Phys. Rev. B **32**, 447 (1985).
- [32] A. Pelissetto and E. Vicari, Off-equilibrium scaling behaviors driven by time-dependent external fields in three-dimensional  $O(N)$  vector models, Phys. Rev. E **93**, 032141 (2016).
- [33] A. W. Sandvik and J. Kurlijärvi, Quantum Monte Carlo simulation method for spin systems, Phys. Rev. B **43**, 5950 (1991).
- [34] O. F. Syljuåsen and A. W. Sandvik, Quantum Monte Carlo with directed loops, Phys. Rev. E **66**, 046701 (2002).
- [35] A. Dorneich and M. Troyer, Accessing the dynamics of large many-particle systems using the stochastic series expansion, Phys. Rev. E **64**, 066701 (2001).